

Estimating the urban heat-related mortality burden due to greenness: a global modelling study



Yao Wu, Bo Wen, Tingting Ye, Wenzhong Huang, Yanming Liu, Antonio Gasparrini, Francesco Sera, Shilu Tong, Eric Lavigne, Dominic Roye, Souzana Achilleos, Niilo Rytty, Mathilde Pascal, Ariana Zeka, Francesca de' Donato, Susana das Neves Pereira da Silva, Joana Madureira, Malcolm Mistry, Ben Armstrong, Michelle L Bell, Joel Schwartz, Yuming Guo, Shanshan Li, on behalf of the MCC Collaborative Research Network*

Summary

Background Heat exposure poses a substantial public health threat. Increasing greenness has been suggested as a mitigation strategy due to its cooling effect and potential to modify the heat–mortality association. This study aimed to comprehensively estimate the effects of increased greenness on heat-related deaths.

Methods We applied a multistage meta-analytical approach to estimate the potential reduction in global heat-related deaths by increasing greenness in the warm season in 2000–19 in 11 534 urban areas. We used the enhanced vegetation index (EVI) to indicate greenness and a random forest model to predict daily temperatures in counterfactual EVI scenarios. In the factual EVI scenarios, daily mortality and weather variables from 830 locations in 53 countries were extracted from the Multi-Country Multi-City Collaborative Research Network and used to assess heat–mortality associations. These associations were then extrapolated to each urban area under both factual and counterfactual EVI scenarios based on meta-regression models.

Findings We estimated that EVI increased by 10% would decrease the global population-weighted warm-season mean temperature by 0.08°C, EVI increased by 20% would decrease temperature by 0.14°C, and EVI increased by 30% would decrease temperature by 0.19°C. In the factual scenario, 3 153 225 (2.48%) of 127 179 341 total deaths could be attributed to heat exposure. The attributable fraction of heat-related deaths (as a fraction of total deaths) in 2000–19 would decrease by 0.67 (95% empirical CI 0.53–0.82) percentage points in the 10% scenario, 0.80 (0.63–0.97) percentage points in the 20% scenario, and 0.91 (0.72–1.10) percentage points in the 30% scenario, compared with the factual scenario. South Europe was modelled to have the largest decrease in attributable fraction of heat-related mortality.

Interpretation This modelling study suggests that increased greenness could substantially reduce the heat-related mortality burden. Preserving and expanding greenness might be potential strategies to lower ambient temperature and reduce the health impacts of heat exposure.

Funding Australian Research Council and Australian National Health and Medical Research Council.

Copyright © 2025 The Author(s). Published by Elsevier Ltd. This is an Open Access article under the CC BY-NC 4.0 license.

Introduction

Heat exposure is a major public health threat^{1–4} and the mortality burden attributable to heat has been increasing in the past two decades.^{5,6} In 2000–19, heat exposure was associated with 0.5 million deaths per year, accounting for 0.91% of global mortality.⁵ Climate change is expected to further exacerbate this issue, with projections in 23 countries indicating that heat-related excess mortality could increase from 0.3–1.7% in the 2010s to 2.5–16.7% in the 2090s in the most extreme global warming scenarios.⁷

Increasing greenness (ie, vegetational land cover, such as grasses, trees, and other plants) has been proposed to reduce the adverse health effects of heat. Previous studies have suggested that greenness has a cooling effect on temperature, achieved by shading surfaces, deflecting radiation from the sun, and evapotranspiration, which promotes air convection.^{8–11}

This cooling effect on temperature results in a decrease in population heat exposure, thereby reducing the heat-related mortality burden. Emerging evidence has also shown that increased greenness could improve heat-related mortality risk,^{12–15} which is potentially related to factors such as mental health, social engagement, physical activity, and air pollution.¹²

To evaluate the effect of greenness on heat-related mortality burden, it is essential to consider both its modification effect on heat-related mortality risk and its influence on daily temperatures. However, previous studies often investigated the two factors separately and have primarily focused on heat-related mortality risk, resulting in a potential underestimation of the protective effects of greenness.^{8,12,16} Questions remain about the extent to which an increase in greenness can offset excess deaths associated with heat exposure. A global assessment of the heat-related mortality

Lancet Planet Health 2025

Published Online

April 30, 2025

[https://doi.org/10.1016/S2542-5196\(25\)00062-2](https://doi.org/10.1016/S2542-5196(25)00062-2)

[S2542-5196\(25\)00062-2](https://doi.org/10.1016/S2542-5196(25)00062-2)

*Members of the MCC

Collaborative Research Network are listed at the end of the Article

Climate, Air Quality Research Unit, School of Public Health and Preventive Medicine, Monash University, Melbourne, VIC, Australia (Y Wu MSc, B Wen MSc, T Ye PhD,

W Huang PhD, Y Liu PhD,

Prof Y Guo PhD, Prof S Li PhD);

Environment & Health Modelling Lab

(Prof A Gasparrini PhD,

M Mistry PhD), Department of Public Health

(Prof B Armstrong PhD),

Environments and Society,

London School of Hygiene & Tropical Medicine, London, UK;

Department of Statistics,

Computer Science and

Applications “G Parenti”,

University of Florence, Florence,

Italy (F Sera PhD); National

Institute of Environmental

Health, Chinese Center for

Disease Control and Prevention,

Beijing, China (Prof S Tong PhD);

School of Public Health and

Social Work, Queensland

University of Technology,

Brisbane, QLD, Australia

(Prof S Tong); School of

Epidemiology & Public Health,

Faculty of Medicine, University

of Ottawa, Ottawa, ON, Canada

(Prof E Lavigne PhD);

Environmental Health Science

and Research Bureau, Health

Canada, Ottawa, ON, Canada

(Prof E Lavigne); Biological

Mision of Galicia (MBG),

Spanish Council for Scientific

Research (CSIC), Madrid, Spain

(D Roye PhD); Climate Research

Foundation (FIC), CIBER of

Epidemiology and Public

Health, Madrid, Spain (D Roye);

Department of Primary Care

and Population Health,

University of Nicosia Medical

School, Nicosia, Cyprus

(S Achilleos PhD); Center for

Environmental and Respiratory Health Research (CERH) and Medical Research Center Oulu (MRC Oulu), University of Oulu, Oulu, Finland (N Ryti PhD); Santé Publique France, Department of Environmental and Occupational Health, French National Public Health Agency, Saint Maurice, France (M Pascal PhD); UK Health Security Agency, London, UK (A Zeka PhD); Department of Epidemiology, Lazio Regional Health Service, ASL Roma 1, Rome, Italy (F de' Donato PhD); Department of Epidemiology (S das Neves Pereira da Silva MSc) and Department of Environmental Health (J Madureira PhD), Instituto Nacional de Saúde Dr Ricardo Jorge, Lisbon, Portugal; EPIUnit, Instituto de Saúde Pública, Universidade do Porto, Porto, Portugal (J Madureira); Laboratório para a Investigação Integrativa e Translacional em Saúde Populacional, Porto, Portugal (J Madureira); Department of Economics, Ca' Foscari University of Venice, Venice, Italy (M Mistry); School of the Environment, Yale University, New Haven, CT, USA (Prof M L Bell PhD); School of Health Policy and Management, College of Health Sciences, Korea University, Seoul, South Korea (Prof M L Bell); Department of Environmental Health, Harvard T H Chan School of Public Health, Boston, MA, USA (Prof J Schwartz PhD)

Correspondence to: Prof Yuming Guo, Climate, Air Quality Research Unit, School of Public Health and Preventive Medicine, Monash University, Melbourne, VIC 3004, Australia yuming.guo@monash.edu

or

Prof Shanshan Li, Climate, Air Quality Research Unit, School of Public Health and Preventive Medicine, Monash University, Melbourne, VIC 3004, Australia shanshan.li@monash.edu

For more on the MCC Collaborative Research Network see <http://mccstudy.lshrm.ac.uk/>

See Online for appendix

For more on Global Human Settlement Layer see <https://human-settlement.emergency.copernicus.eu/>

Research in context

Evidence before this study

Heat exposure poses a substantial public health threat. Increasing greenness has been proposed as a mitigation strategy due to its cooling effect on temperature and potential to modify the heat-mortality association. To accurately evaluate this impact, it is essential to consider both the modifying and cooling effects of greenness. We searched MEDLINE, Embase, Web of Science, Scopus, and PubMed for studies published from database inception to Dec 30, 2023, using search terms related to heat, greenness, and mortality. Although many studies have explored these relationships, previous studies often investigated the two factors separately, potentially underestimating the protective effects of greenness. For example, a study of 452 locations in 24 countries, a subset of the locations used in this study, only considered the modifying role of greenness on the heat-mortality relationship, without accounting for its cooling effects on temperatures. Another study in Europe examined the cooling effects of urban tree coverage, but not its modifying effect on the heat-mortality relationship.

Added value of this study

To the best of our knowledge, this is the first modelling study to estimate the global urban heat-related mortality burden that could be prevented by increasing the enhanced vegetation index (EVI) in 2000–19. By considering both the cooling and

burden prevented by increasing greenness could provide valuable insights into the development of practical and context-specific strategies for mitigating adverse health effects associated with heat.

This study aimed to evaluate the potential reduction in heat-related deaths across global urban areas by increasing greenness to different levels, considering both the modifying role of greenness on the heat-mortality relationship and the cooling effect of greenness on daily temperatures.

Methods

Data collection

This multistage meta-analytical modelling study was conducted by the Multi-Country Multi-City (MCC) Collaborative Research Network, which was developed in 2014 to produce epidemiological evidence on associations between environmental stressors, climate, and health across countries and regions using a unified and standardised methodology.¹⁷ In this study, daily mortality and weather variables were extracted from 830 locations in 53 countries (appendix pp 9–10, 12). ICD-9 and ICD-10 codes were used to identify causes of death. Data series on non-external causes of death were extracted (ICD-9 codes 0–799; ICD-10 codes A00–R99), or, if not available, all-cause mortality. Mean daily temperatures were obtained from ground monitoring stations and calculated as the average between daily

modifying effects of greenness, this study provides a more comprehensive assessment of its benefits in mitigating heat-related mortality. Our analysis, which includes 11 534 urban areas at high resolution, enhances the generalisability of the findings. Our model found that that increasing EVI levels by 10–30% would decrease the global population-weighted warm-season mean temperature and prevent 0.86–1.16 million heat-related deaths. The effects of EVI on heat-related mortality vary across urban areas with different climate types, greenness levels, socioeconomic statuses, and demographic characteristics.

Implications of all the available evidence

This study suggests that increased greenness could significantly reduce the heat-related mortality burden. These findings indicate that preserving and expanding greenness might be potential strategies to lower temperature and mitigate the health impacts of heat exposure. The global spatial pattern of prevented heat-related mortality due to greenness presented in this study helps us to understand the heterogeneity of the effects across urban areas with different climate types, greenness levels, socioeconomic statuses, and demographic characteristics. This evidence provides insights for policy makers to design and implement tailored green initiatives that enhance public health and foster sustainable, heat-resilient urban environments.

maximum and minimum values or the 24-h average based on hourly measurements. Detailed information on data collection and cleaning is described in the appendix (pp 3, 4).

A total of 11 534 urban areas with geographical boundaries obtained from the Global Human Settlement Layer project¹⁸ were included in our analyses. An urban area was defined as an area with a density of at least 1500 inhabitants per km² of permanent land and a total population of over 50 000.¹⁹ The geographical size of these urban areas varies widely, ranging from relatively small areas (~1 km²) to large metropolitan areas (~6611 km²).

For both greenness and meteorological data, the mean values of all grid cells (ie, pixels covering the boundary of each location or urban area) were calculated to represent the environmental exposures. This method ensured spatially representative data for each location or urban area.

We measured greenness through the enhanced vegetation index (EVI), which is a satellite-image-based vegetation index derived from the Moderate Resolution Imaging Spectroradiometer (MODIS) product, MOD13Q1, collected from the National Aeronautics and Space Administration's Terra satellite.^{20,21} MOD13Q1 data have been available at a spatial resolution of 250×250 m every 16 days since 2000. These 16-day composites were generated on a per-pixel basis using the constrained view

angle–maximum value composite algorithm. This algorithm selects the best observations within 16 days, minimising the effects of image quality, cloud cover, and view angle. EVI is a modified vegetation index and therefore has improved sensitivity in regions with high biomass and a higher vegetation monitoring capability; it is calculated by the following formula:

$$EVI = G \frac{NIR - Red}{NIR + C1Red - C2Blue + L}$$

where the near-infrared radiation (NIR), red (Red) reflectance, and blue (Blue) reflectance are the full or partly atmospheric-corrected surface reflectances; G is a scaling factor; L is the canopy background adjustment; and C1 and C2 are the coefficients of the aerosol resistance term. The parameters for MOD13Q1 are set to L is 1, C1 is 6, C2 is 7.5, and G is 2.5.²² The monthly mean EVI values were calculated by averaging the 16-day EVI composites within each month. We excluded negative EVI values in all pixels to ensure that negative values (indicating non-vegetated surfaces) would not offset positive values in calculating the monthly and area mean values. We linked monthly EVI values with each location or urban area using the mean pixel values covering the boundaries of the location.

Hourly meteorological data were obtained from the fifth-generation European Centre for Medium-Range Weather Forecasts Reanalysis (ERA5), at a spatial resolution of 0.1° latitude by 0.1° longitude.²³ The hourly records were used to calculate daily meteorological parameters according to the local time zone of each grid cell. These daily meteorological parameters included: daily mean ambient temperature (at a height of 2 m above the surface of the Earth), daily mean eastward component of the 10 m wind (at a height of 10 m above the surface of the Earth), daily mean northward component of the 10 m wind, daily total precipitation, daily mean pressure (force per unit area) of the atmosphere at the surface of land, sea, and inland water, and daily mean downward solar radiation at the surface. The daily meteorological values were linked to each urban area by calculating the mean values of all grid cells covering the boundary of the urban area or location.

Global gross domestic product (GDP) per capita data were obtained by combining population data and GDP data from the Global Carbon Project at a 0.5° grid resolution (ie, 0.5° latitude by 0.5° longitude) every 10 years from 1980 to 2020. Population and GDP data were linearly interpolated over time to generate annual values. GDP per capita was then calculated by dividing GDP by population for each grid cell and assigned to each urban area or location using the value of the grid cell covering the centroid of the urban area or location.

To calculate the baseline daily death counts for each urban area, we obtained country-specific mortality rates for each year from the World Bank and population data

from LandScan Global at a 30 arc-second (approximately 1 km) resolution from 2000 to 2019. For each year, the total population count for each urban area was calculated as the sum of the values of grid cells covering the boundary of the urban area or location. The mean daily deaths for each urban area were computed by multiplying the annual mortality rate of the country where the urban area was located with the total population of the urban area, further divided by the number of days of the year.

Statistical analysis

We used a multistage modelling framework to estimate the change in global urban heat-related mortality burden attributable to increased greenness. In stage 1, we applied a random forest model to predict counterfactual daily temperatures in different EVI scenarios, capturing the cooling effect of greenness on ambient temperature. In stage 2, we estimated location-specific heat–mortality associations using distributed lag non-linear models based on daily temperature and mortality data. In stage 3, these associations were extrapolated to all urban areas using a meta-regression model,^{5,24} in which EVI was included as a predictor along with climate type, socioeconomic status, and other factors, to account for its modifying effect on heat-related mortality risk. In stage 4, we calculated heat-attributable mortality in both factual and counterfactual EVI scenarios using the factual or counterfactual temperatures and the corresponding exposure–response relationships. By integrating both the cooling and modifying effects of greenness, this framework provides a comprehensive assessment of its potential to mitigate heat-related mortality risks on a global scale.

To estimate counterfactual daily temperatures in different EVI scenarios in stage 1, we applied a random forest model to correlate factual daily temperatures with monthly EVI at the urban area level, recognising that urban greenness typically remains stable within a given season. Several predictors were also considered in the random forest model, including daily mean eastward and northward components of 10 m wind, daily total precipitation, daily mean surface air pressure, daily mean downward solar radiation at the surface, longitude, latitude, region, year, and month. The indicator variable for region had 15 categories, including North Europe, South Europe, West Europe, East Europe, North America, Latin America and the Caribbean, North Africa, Sub-Saharan Africa, Central Asia, South Asia, West Asia, East Asia, Southeast Asia, Australia and New Zealand, and other regions in Oceania. Our model reached a high level of accuracy in estimating daily temperature (average R²=0.93; average root mean squared error 1.37°C; appendix p 11). All projected temperature series were further calibrated using the factual temperature series. Detailed information on the random forest model is provided in the appendix (pp 4, 5). The trained random forest model was used to predict daily mean temperature

For more on LandScan Global see <https://www.eastview.com/resources/e-collections/landscan/>

For more on the Global Carbon Project see <https://www.globalcarbonproject.org>

for each urban area in four counterfactual EVI scenarios: EVI decreased to 0, EVI increased by 10%, EVI increased by 20%, and EVI increased by 30%, relative to the baseline EVI values of each urban area. The scenario where EVI values decreased to 0 represents the complete loss of current vegetative cover.

In stage 2, a generalised linear regression model with a quasi-Poisson family was applied in each of the 830 locations to estimate location-specific heat–mortality associations. We used distributed lag non-linear models to model the non-linear and lagged effects of daily mean temperature during the warm season, defined as the hottest consecutive 4 months. The distributed lag non-linear model built a 2D cross-basis function of daily mean temperature, with one dimension featuring the non-linear effect of temperature and the other dimension for lag. The temperature dimension includes a natural spline function with two internal knots placed at the 50th and 90th percentiles of the location-specific warm-season temperature distribution. The lag dimension is modelled with a natural spline function with two internal knots at equally spaced values in the log scale over 10 days of lag. Seasonality was modelled by including the day of year as a variable with a natural spline function of four degrees of freedom. We also included an interaction between the seasonality spline and year to allow for different seasonal trends across the study period. Additionally, we included a natural spline function of time with approximately one knot every 10 years to control for long-term trends. The model also included a categorical variable for day of the week. These parameters were chosen based on previous studies.^{3,25} Detailed information on the location-specific exposure–response associations is provided in the appendix (pp 5, 6).

Stage 3 used a multivariate meta-regression prediction model to estimate the relationship between heat-related mortality risk and various explanatory variables, including EVI, continents, Köppen–Geiger climate classification indicators, GDP per capita, the yearly average of daily mean temperature, and the range of daily mean temperature. The choice of explanatory variables is based on their established relevance to the heterogeneity of temperature-related mortality risk and related global studies from the MCC Collaborative Research Network.^{5,24,26} The EVI was incorporated into the meta-regression model to examine the modifying effect of greenness on the heat–mortality relationship, allowing us to illustrate response patterns across different EVI levels. The performance of the model improved substantially with the addition of EVI ($p < 0.05$). We calculated mid-year GDP per capita and EVI to reflect the average level of GDP per capita and EVI for each location during the study period. Continents included the Americas, Europe, Africa, Asia, and Oceania. The climate classification was based on the Köppen–Geiger system and represented by an indicator variable with five categories: group A (tropical climates), group B

(arid climates), group C (temperate climates), group D (continental climates), and group E (polar and alpine climates).^{27,28} We used the fitted meta-regression model with urban area-specific explanatory variables to estimate the heat–mortality association in 2000–19 for each urban area in both counterfactual and factual EVI scenarios. The minimum mortality temperature is the temperature at which the risk of mortality is lowest and is specific to each location. We derived the minimum mortality temperature for each urban area based on the cumulative exposure–response curve represented by the heat–mortality association for that urban area.

To estimate the heat-related deaths and attributable fractions of heat-related mortality in different EVI scenarios in stage 4, we used a method described elsewhere.²⁹ Specifically, for each urban area, day, and scenario, we calculated the number of heat-related deaths based on the counterfactual temperature series, daily mortality, and the urban-scenario-specific heat–mortality associations obtained in stage 3. We then estimated the total number of heat-related deaths in each urban area and scenario from 2000 to 2019 by summing the heat-related deaths for the days when the temperature was higher than the urban-specific minimum mortality temperatures. To calculate the attributable fraction of heat-related mortality for each urban area and scenario, we divided the total heat-related deaths by the total number of deaths. We used Monte Carlo simulations to generate 1000 samples of the coefficients to quantify the uncertainty of the estimates. The 2.5th and 97.5th percentiles of these distributions are interpreted as 95% empirical confidence intervals (eCIs). Heat-related deaths and attributable fractions were aggregated at the country, region, continent, and global levels. We calculated the change in heat-related deaths and attributable fraction of heat-related deaths by increasing EVI as the difference compared with the factual EVI scenario. The details on the calculation of heat-related deaths and attributable fractions are provided in the appendix (pp 6, 7).

To assess the potential modification effects of urban characteristics, we performed several stratified analyses based on climate type (Köppen–Geiger climate classification), greenness level (EVI), socioeconomic status (GDP per capita and human development index), and demographic characteristics (proportion of children younger than 5 years or population aged 65 years and older). We classified urban areas into subgroups according to these characteristics and calculated the changes in attributable fractions of heat-related deaths in each counterfactual scenario compared with the factual scenario (appendix pp 7, 8). We also conducted sensitivity analyses using absolute changes in EVI scenarios instead of relative changes. Specifically, we established three alternative scenarios by increasing EVI levels to the 50th, 60th, and 70th percentiles of the global urban EVI distribution in 2019. Consequently, only urban areas with

original EVI levels below these cutoff values were included in the sensitivity analyses.

Role of the funding source

The funders had no role in study design, data collection, data analyses, data interpretation, or writing of this report.

Results

In our modelling framework, EVI increased by 10% was estimated to decrease the global population-weighted warm-season mean temperature by 0.08°C, EVI increased by 20% had an estimated decrease of 0.14°C, EVI increased by 30% had an estimated decrease of 0.19°C, and EVI decreased to 0 had an estimated increase of 0.23°C (figure 1; appendix p 13). West Europe would have had the largest reduction in population-weighted warm-season mean temperature, with decreases of 0.17°C in the 10% scenario, 0.30°C in the 20% scenario, and 0.39°C in the 30% scenario. North Africa, East Asia, and other regions in Oceania would have had the least reduction in population-weighted warm-season mean temperature, with a decrease of less than 0.03°C in all three EVI-increasing scenarios. Most regions were modelled to have an increase in temperature if EVI decreased to 0, except for East Europe and Latin America and the Caribbean.

In the factual scenario, 3 153 225 (2.48%) of 127 179 341 total deaths could be attributed to heat exposure in 2000–19 (table 1). Increasing EVI by 10% was estimated to prevent 0.86 million (95% eCI 0.67–1.05) global heat-related deaths in 2000–19, EVI increased by 20% to prevent 1.02 million (0.81–1.23) deaths, and EVI increased by 30% to prevent 1.16 million (0.92–1.40) deaths. Higher percentage increases in EVI were modelled to reduce heat-related death across most regions, with the exceptions of North Africa and other regions in Oceania in any of the three EVI scenarios (table 1; appendix p 14). Country-specific heat-related deaths are provided in the appendix (pp 15–18).

Globally, the attributable fraction of heat-related deaths was estimated to decrease by 0.67 (95% eCI 0.53 to 0.82) percentage points in the 10% scenario, 0.80 (0.63 to 0.97) percentage points in the 20% scenario, and 0.91 (0.72 to 1.10) percentage points in the 30% scenario, compared with the factual scenario (figure 2). By contrast, the global fraction of heat-related death was estimated to increase by 0.51 (–0.08 to 1.04) percentage points if EVI decreased to 0. South Europe was modelled to have the largest absolute decrease in attributable fraction of heat-related deaths, with decreases of 1.94 (1.79 to 2.10) percentage points in the 10% scenario, 2.23 (2.08 to 2.40) percentage points in the 20% scenario, and 2.47 (2.30 to 2.66) percentage points in the 30% scenario. However, North America and Latin America and the Caribbean were modelled to have significant absolute decreases in attributable fraction of heat-related deaths if EVI decreased to 0. The relative decreases in attributable

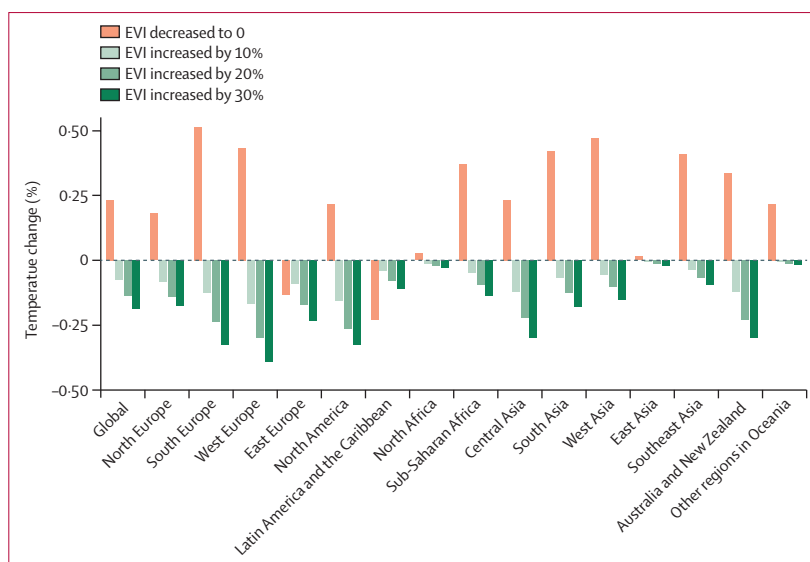


Figure 1: Modelled change in population-weighted warm-season mean temperature under different EVI scenarios compared with the factual scenario in 2000–19 by region and continent

The model reached a high level of accuracy in estimating daily temperature (average $R^2=0.93$; average root mean squared error 1.37°C; appendix p 11). EVI=enhanced vegetation index.

fraction of heat-related deaths at global and regional levels are reported in the appendix (p 19): at the global level, there was a modelled decrease of 27.16 (21.79 to 35.53) percentage points in the 10% scenario, 32.22 (26.89 to 40.44) percentage points in the 20% scenario, and 36.66 (31.32 to 44.80) percentage points in the 30% scenario. The largest relative decreases in the 30% scenario were modelled for Australia and New Zealand (reduction of 82.98% [41.46 to 503.34]), North Europe (reduction of 67.53% [60.34 to 74.58]), and North America (62.89% [54.10 to 79.02]; appendix p 19). North Africa and other regions in Oceania were modelled to have an increase in attributable fraction in heat-related deaths in all counterfactual scenarios, although the estimates are not statistically significant. The country-specific changes in the attributable fraction of heat-related deaths are shown in the appendix (pp 20–22).

Figure 3 presents the modelled change in attributable fraction of heat-related deaths for the top 1000 most populated urban areas. Most of the urban areas that have the largest modelled reductions in attributable fraction of heat-related deaths compared with the factual scenario (ie, changes $\geq 1\%$) are located in Europe and Latin America across all three EVI-increasing scenarios. In contrast, nearly all urban areas modelled to have an increase in heat-related deaths in the counterfactual scenarios are in Africa. When EVI was decreased to 0, 613 (61%) of the top 1000 most populated urban areas were modelled to have an increase in attributable fractions of heat-related deaths, and 248 (25%) of these locations had increases in heat-related death of 1% or higher, with the majority in Africa, West Europe, South Asia, and Southeast Asia.

	Heat-related deaths in factual scenario	Modelled change in heat-related deaths			
		EVI decreased to 0	EVI increased by 10%	EVI increased by 20%	EVI increased by 30%
Global	3 153 225 (2 277 540 to 3 923 289)	644 039 (-107 707 to 1 324 699)	-856 311 (-1 048 573 to -667 718)	-1 015 829 (-1 229 646 to -805 006)	-1 155 920 (-1 395 185 to -917 477)
Europe	883 217 (746 305 to 1 003 285)	54 227 (-76 397 to 176 229)	-307 588 (-339 439 to -276 088)	-358 263 (-392 363 to -323 547)	-396 955 (-436 017 to -357 367)
North Europe	48 916 (35 703 to 61 008)	10 243 (-22 491 to 41 808)	-28 834 (-38 241 to -19 197)	-31 294 (-40 812 to -21 629)	-33 031 (-42 666 to -23 204)
South Europe	200 749 (172 871 to 224 345)	16 721 (-4490 to 36 388)	-70 536 (-76 284 to -64 914)	-81 198 (-87 052 to -75 469)	-89 940 (-96 588 to -83 423)
West Europe	111 612 (94 912 to 125 835)	44 176 (9199 to 77 579)	-50 254 (-53 190 to -46 902)	-59 377 (-63 538 to -54 615)	-65 696 (-70 841 to -59 686)
East Europe	521 940 (442 819 to 592 097)	-16 913 (-58 613 to 20 454)	-157 963 (-171 724 to -145 075)	-186 394 (-200 961 to -171 833)	-208 288 (-225 921 to -191 053)
Americas	383 354 (238 291 to 505 495)	-123 829 (-182 936 to -65 227)	-156 529 (-193 226 to -118 228)	-177 150 (-214 727 to -139 366)	-192 392 (-235 555 to -149 044)
North America	110 199 (74 359 to 141 804)	-26 810 (-51 215 to -4726)	-58 017 (-70 294 to -45 985)	-64 777 (-78 808 to -50 764)	-69 306 (-84 066 to -54 029)
Latin America and the Caribbean	273 154 (163 931 to 363 691)	-97 018 (-131 721 to -60 501)	-98 512 (-122 932 to -72 243)	-112 373 (-135 919 to -88 602)	-123 085 (-151 489 to -95 014)
Africa	145 857 (36 938 to 241 030)	219 054 (32 473 to 389 066)	-9 720 (-41 607 to 20 222)	-20 644 (-57 323 to 15 060)	-35 853 (-76 687 to 5244)
North Africa	24 459 (8195 to 38 868)	18 279 (4565 to 30 823)	2143 (-1464 to 5770)	1386 (-2650 to 5273)	430 (-3286 to 4211)
Sub-Saharan Africa	121 398 (28 743 to 202 162)	200 775 (27 908 to 358 243)	-11 863 (-40 143 to 14 452)	-22 030 (-54 672 to 9787)	-36 283 (-73 401 to 1033)
Asia	1 737 501 (1 257 265 to 2 166 322)	494 154 (121 958 to 821 296)	-380 094 (-469 888 to -293 586)	-457 174 (-560 759 to -356 789)	-527 989 (-642 296 to -415 865)
Central Asia	23 568 (16 291 to 30 245)	-1663 (-6066 to 2491)	-8347 (-10 793 to -5861)	-9 520 (-12 166 to -7050)	-10 473 (-13 223 to -7825)
South Asia	794 732 (596 773 to 967 306)	314 976 (161 876 to 448 734)	-155 726 (-186 662 to -126 081)	-200 123 (-237 978 to -163 042)	-240 198 (-283 991 to -197 295)
West Asia	126 661 (95 478 to 153 845)	7046 (-8226 to 20 677)	-28 298 (-36 076 to -20 634)	-31 437 (-40 365 to -23 210)	-34 978 (-43 927 to -26 253)
East Asia	608 622 (435 622 to 769 534)	-10 085 (-111 286 to 79 525)	-126 207 (-160 069 to -93 608)	-141 651 (-177 837 to -106 725)	-156 677 (-194 114 to -120 205)
Southeast Asia	183 918 (113 100 to 245 392)	183 879 (85 659 to 269 869)	-61 516 (-76 289 to -47 402)	-74 443 (-92 413 to -56 762)	-85 662 (-107 041 to -64 287)
Oceania	3297 (-1258 to 7157)	433 (-2805 to 3335)	-2380 (-4414 to -38)	-2598 (-4474 to -364)	-2733 (-4630 to -446)
Australia and New Zealand	3325 (-1151 to 7116)	591 (-2175 to 3250)	-2407 (-4377 to -138)	-2624 (-4433 to -467)	-2759 (-4591 to -548)
Other regions in Oceania	-28 (-107 to 41)	-158 (-630 to 85)	27 (-37 to 101)	27 (-42 to 102)	27 (-39 to 102)

Data are n (95% eCI). eCI=empirical confidence interval. EVI=enhanced vegetation index.

Table 1: Modelled change in heat-related deaths in different EVI scenarios compared with the factual scenario in 2000–19 by region and continent

Table 2 shows that the modelled change in attributable fraction of heat-related deaths in different EVI scenarios was potentially modified by climate type, greenness level, socioeconomic status, and demographic characteristics. Urban areas with a continental climate were modelled to have the largest reduction in attributable fraction of heat-related deaths, whereas those with a polar climate had the smallest reduction. Generally, the modelled reduction in attributable fraction of heat-related deaths increased with higher factual EVI levels, except in urban areas with the highest greenness levels (the high group). Urban

areas with higher socioeconomic status—higher GDP per capita or higher human development index (HDI)—were modelled to have a larger reduction in attributable fraction of heat-related deaths than those with lower socioeconomic status. Furthermore, urban areas with fewer children younger than 5 years or a higher proportion of people aged 65 years and older also showed greater reductions in attributable fraction of heat-related deaths.

Sensitivity analyses by using absolute changes in EVI scenarios instead of relative changes show that the main

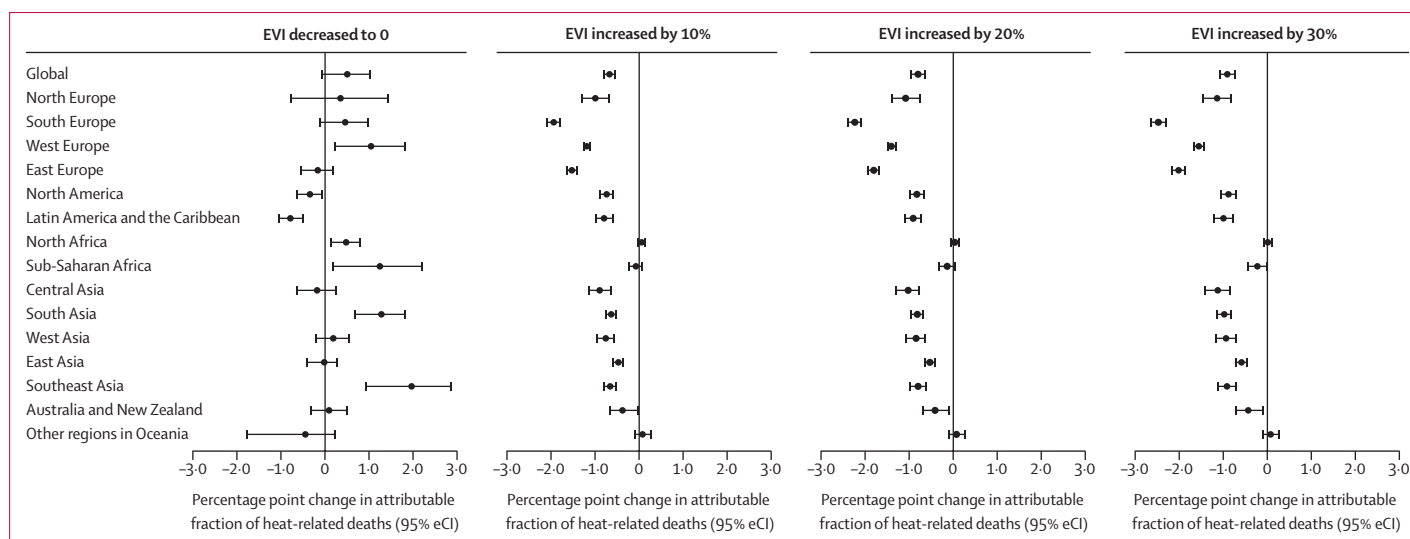


Figure 2: Modelled change in attributable fraction of heat-related deaths in different enhanced vegetation index scenarios compared with the factual scenario in 2000–19
Data are percentage point change in the attributable fraction of heat-related deaths with 95% eCI. To calculate the attributable fraction of heat-related deaths, the total number of heat-related deaths was divided by the total number of deaths. eCI=empirical confidence interval. EVI=enhanced vegetation index.

results were still robust when increasing EVI levels to the 50th, 60th, and 70th percentiles of the global EVI distribution (appendix pp 23–25).

Discussion

To the best of our knowledge, this is the first study to use a counterfactual model to estimate the global urban heat-related mortality burden that could be prevented by increasing EVI to different levels. Our model showed that increasing EVI by 10–30% would result in a global average decrease in warm-season population-weighted mean temperature of 0.08–0.19°C and prevent 0.86–1.16 million deaths compared with the counterfactual scenario in 2000–19. The effect of increased EVI varied geographically, with urban areas in South Asia, East Europe, and East Asia modelled to have the greatest absolute reductions in heat-related deaths.

Our findings show that increasing EVI could significantly reduce global heat-related deaths. This finding is supported by previous studies on the effect of greenness on the temperature–mortality association, which have shown that greenness can protect against heat-related mortality from all causes, diabetes, and stroke.^{12,16,30–32} However, most previous studies have been limited to single countries or regions, particularly in South Asia and East Asia, so the role of greenness in other regions is still unknown. One study of 452 locations in 24 countries, a subset of the locations used in this study, found that a 1–20% increase in normalised difference vegetation index was associated with a 0.5–9% reduction in heat-related mortality.¹² The estimates of that study are lower than our estimates, possibly because it only considered the modifying role of greenness on the exposure–response curve between heat and mortality, and not the cooling effects of greenness on daily temperatures.

Our findings suggest that the effects of EVI on heat-related mortality vary across urban areas with different regions, climate types, greenness levels, socioeconomic statuses, and demographic characteristics. This variation can be attributed to the combination of the difference in the cooling effect of greenness on temperature and the difference in the modifying effect of greenness on heat-related mortality.

Greenness influences temperature through biogeophysical (eg, albedo, evapotranspiration) and biogeochemical (eg, CO₂ absorption) processes.³³ Although urban vegetation typically cools the environment through shading and evapotranspiration, it can also lower surface albedo, leading to increased heat retention.³³ For most urban areas included in this study, the cooling effect of greenspace dominated the counterbalance of these two effects. However, contrary to expectations, we also found that a complete loss of greenness was associated with a temperature decrease in East Europe and Latin America and the Caribbean. This finding might be attributed to variations in the cooling efficacy of greenspace across different climate types. East Europe has a predominantly continental climate, where deforestation can induce cooling due to the substantial albedo contrast between forest canopies and snow-covered surfaces.³⁴ By contrast, in most tropical climates (eg, Southeast Asia), deforestation commonly exerts a warming effect due to a decrease in absorbing CO₂ and a decrease in evapotranspiration.³⁴ However, for some urban areas in Latin America and the Caribbean, in the cases of extreme heat and high background humidity, transpiration cooling becomes less effective.³⁵ Additionally, dense tree canopies can trap long-wave radiation at night, potentially elevating temperatures.³⁵ Consequently, vegetation loss in these regions might lead to a slight cooling effect. Furthermore,

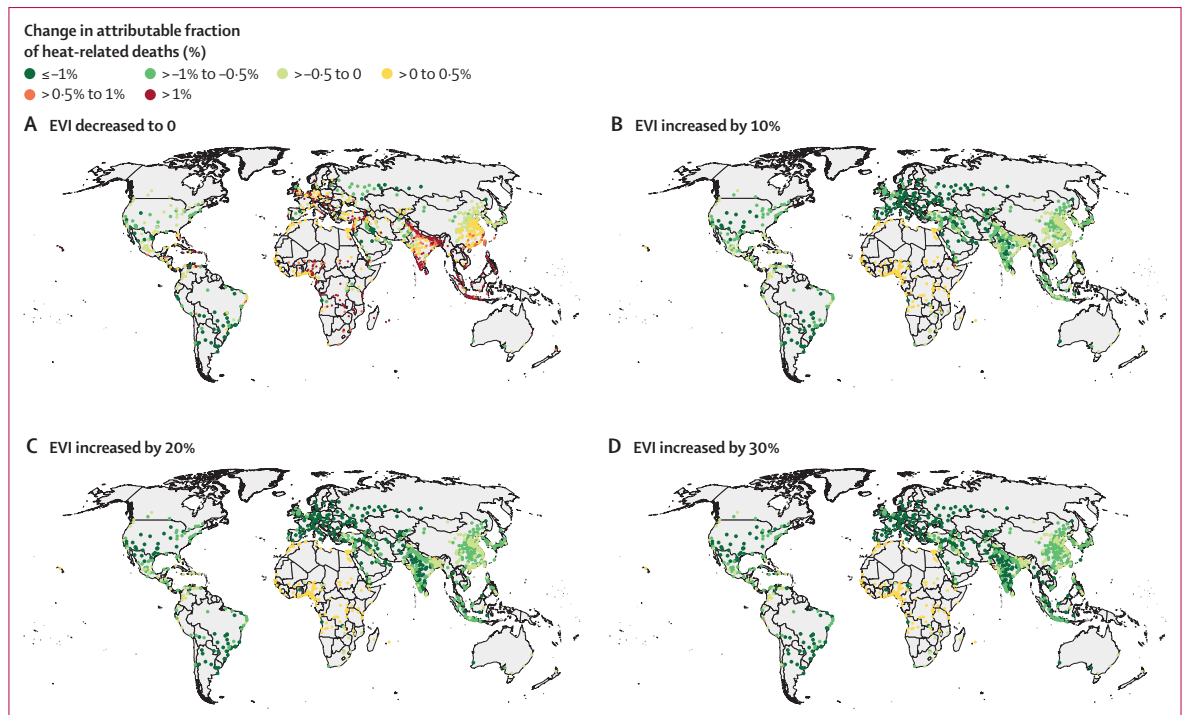


Figure 3: Modelled change in attributable fraction of heat-related deaths in different EVI scenarios in 2000–19 for the top 1000 most populated urban areas. To calculate the attributable fraction of heat-related deaths, the total number of heat-related deaths was divided by the total number of deaths. EVI=enhanced vegetation index.

large-scale deforestation in surrounding areas can modify moisture transport and cloud formation, reducing incoming solar radiation and contributing to localised cooling in urban environments.³⁶ Nevertheless, as our results are primarily model driven, further empirical studies are needed to validate these findings and elucidate the underlying mechanisms.

Greenness can also modify the association between heat and mortality, primarily by reducing susceptibility to heat-related health risks. This effect could be mediated through multiple mechanisms, including lowering air pollution and noise levels, as well as enhancing physical activity, social engagement, and mental wellbeing.³⁷ Additionally, greenness influences humidity levels, which can affect both thermal comfort and thermoregulation by altering evaporative heat loss from the skin surface and insensible water loss.³⁸ In this study, we observed an increase in heat-related mortality risk in North America in an EVI decreased to 0 scenario (appendix p 14). However, North America was modelled to have reduced attributable fraction of heat-related deaths in the EVI decreased to 0 scenario. This finding might be partly explained by the non-linear relationship between EVI and ambient temperature. As shown in the appendix (p 14), the heat–mortality relationship of North America follows a J-shaped curve, with a minimum mortality temperature of approximately 23°C. Although the complete loss of greenness is expected to contribute to warming,

most of this temperature increase occurs on days with temperatures below the minimum mortality temperature (population-weighted average temperature change 1·20°C), whereas days with temperatures above the minimum mortality temperature have a slight cooling effect (population-weighted average temperature change –0·65°C). Consequently, despite an overall increase in ambient temperature in the EVI decreased to 0 scenario (figure 1), the estimated heat-related mortality burden decreases, as only temperatures exceeding the minimum mortality temperature contribute to heat-related mortality. The varying effects of EVI on temperature probably result from multiple interacting factors, such as regional climate conditions and vegetation characteristics. However, further research is needed to better understand these complex interactions and their implications for heat-related health risks.

This study observed that urban areas with higher socioeconomic status (measured by GDP per capita or HDI) are more likely to have a greater reduction in attributable fraction of heat-related mortality due to increased greenness. Several factors might explain this pattern. First, urban areas with higher socioeconomic status tend to have higher baseline EVI levels (appendix p 26). As a result, increasing EVI by a specific proportion leads to a larger absolute increase, ultimately enhancing both the cooling and modifying effects of greenness. Second, socioeconomic disparities contribute to

	Attributable fraction (%) in factual scenario	Modelled percentage point change in attributable fraction (95% eCI)			
		EVI decreased to 0	EVI increased by 10%	EVI increased by 20%	EVI increased by 30%
Climate type					
Tropical	1.62 (0.75 to 2.40)	1.39 (0.03 to 2.66)	-0.42 (-0.67 to -0.17)	-0.53 (-0.81 to -0.25)	-0.64 (-0.95 to -0.32)
Arid	3.14 (2.21 to 3.97)	0.07 (-0.43 to 0.56)	-0.67 (-0.95 to -0.40)	-0.80 (-1.10 to -0.50)	-0.94 (-1.25 to -0.62)
Temperate	2.40 (1.82 to 2.92)	0.29 (-0.34 to 0.87)	-0.74 (-0.91 to -0.56)	-0.85 (-1.05 to -0.66)	-0.95 (-1.15 to -0.74)
Continental	3.81 (2.99 to 4.55)	-0.29 (-0.71 to 0.09)	-1.13 (-1.31 to -0.95)	-1.30 (-1.50 to -1.09)	-1.43 (-1.63 to -1.22)
Polar	-1.30 (-12.20 to 7.45)	0.85 (-1.19 to 3.06)	-0.27 (-2.07 to 1.66)	-0.44 (-2.35 to 1.55)	-0.60 (-2.58 to 1.48)
EVI level					
Low (≤ 0.20)	2.60 (1.72 to 3.39)	0.12 (-0.46 to 0.68)	-0.57 (-0.82 to -0.31)	-0.67 (-0.95 to -0.39)	-0.78 (-1.08 to -0.47)
Moderate-low (>0.20 to 0.26)	2.39 (1.66 to 3.06)	0.50 (-0.30 to 1.25)	-0.64 (-0.85 to -0.44)	-0.77 (-0.99 to -0.55)	-0.89 (-1.12 to -0.64)
Moderate-high (>0.26 to 0.31)	2.68 (1.97 to 3.31)	0.47 (-0.32 to 1.20)	-0.87 (-1.06 to -0.67)	-1.03 (-1.27 to -0.79)	-1.15 (-1.40 to -0.90)
High (>0.31)	2.01 (1.37 to 2.59)	1.66 (0.31 to 2.93)	-0.71 (-0.87 to -0.54)	-0.82 (-1.01 to -0.63)	-0.90 (-1.11 to -0.68)
GDP per capita (US\$)					
Low (≤ 1950)	1.78 (0.99 to 2.48)	1.45 (0.12 to 2.70)	-0.25 (-0.47 to -0.03)	-0.38 (-0.65 to -0.10)	-0.50 (-0.80 to -0.19)
Moderate-low (>1950 to 4375)	2.39 (1.60 to 3.11)	1.19 (0.16 to 2.16)	-0.44 (-0.68 to -0.21)	-0.57 (-0.82 to -0.32)	-0.70 (-0.98 to -0.41)
Moderate-high (>4375 to 9216)	2.41 (1.60 to 3.13)	0.60 (-0.14 to 1.27)	-0.61 (-0.83 to -0.40)	-0.71 (-0.95 to -0.48)	-0.81 (-1.06 to -0.55)
High (>9216)	2.73 (1.99 to 3.39)	-0.10 (-0.68 to 0.44)	-0.92 (-1.13 to -0.71)	-1.05 (-1.29 to -0.82)	-1.16 (-1.40 to -0.91)
Human development index					
Low (≤ 0.55)	1.81 (1.02 to 2.52)	1.21 (-0.11 to 2.46)	-0.23 (-0.52 to 0.07)	-0.33 (-0.65 to -0.01)	-0.46 (-0.81 to -0.10)
Medium (>0.55 to 0.70)	2.21 (1.44 to 2.88)	0.88 (0.01 to 1.71)	-0.44 (-0.65 to -0.24)	-0.56 (-0.79 to -0.34)	-0.67 (-0.91 to -0.42)
High (>0.70 to 0.80)	2.78 (1.96 to 3.53)	0.39 (-0.24 to 0.97)	-0.74 (-0.95 to -0.54)	-0.88 (-1.11 to -0.64)	-0.98 (-1.23 to -0.73)
Very high (>0.80)	2.62 (1.92 to 3.25)	0.07 (-0.59 to 0.70)	-0.94 (-1.15 to -0.74)	-1.07 (-1.30 to -0.85)	-1.18 (-1.41 to -0.94)
Children younger than 5 years					
$\leq 6\%$	3.05 (2.33 to 3.69)	0.03 (-0.49 to 0.51)	-0.90 (-1.06 to -0.74)	-1.04 (-1.22 to -0.86)	-1.16 (-1.35 to -0.96)
>6% to 9%	2.14 (1.35 to 2.85)	0.53 (-0.29 to 1.31)	-0.71 (-0.96 to -0.45)	-0.82 (-1.09 to -0.55)	-0.92 (-1.20 to -0.63)
>9% to 12%	2.42 (1.59 to 3.17)	0.94 (0.08 to 1.74)	-0.54 (-0.75 to -0.33)	-0.67 (-0.92 to -0.42)	-0.79 (-1.05 to -0.52)
>12%	1.81 (1.03 to 2.51)	1.07 (-0.25 to 2.31)	-0.23 (-0.52 to 0.06)	-0.33 (-0.66 to 0.00)	-0.45 (-0.81 to -0.08)
Population older than 65 years					
$\leq 4\%$	1.96 (1.11 to 2.73)	1.01 (-0.19 to 2.13)	-0.35 (-0.64 to -0.05)	-0.45 (-0.77 to -0.12)	-0.56 (-0.91 to -0.20)
>4% to 6%	2.34 (1.59 to 3.02)	0.85 (0.05 to 1.60)	-0.51 (-0.70 to -0.32)	-0.63 (-0.86 to -0.41)	-0.74 (-0.99 to -0.50)
>6% to 9%	2.36 (1.56 to 3.08)	0.42 (-0.25 to 1.04)	-0.63 (-0.83 to -0.42)	-0.74 (-0.97 to -0.51)	-0.84 (-1.08 to -0.59)
>9%	2.97 (2.27 to 3.60)	0.05 (-0.56 to 0.62)	-1.01 (-1.20 to -0.81)	-1.15 (-1.36 to -0.94)	-1.27 (-1.49 to -1.04)

Data are percentage point change in attributable fraction of heat-related deaths (95% eCI). eCI=empirical confidence interval. EVI=enhanced vegetation index

Table 2: Modelled change in attributable fraction of heat-related deaths in different EVI scenarios compared with the factual scenario by climate type, greenness level, socioeconomic status, and demographic characteristics

differences in heat vulnerability.^{39–41} Wealthier areas were observed to have a higher baseline heat–mortality association (appendix p 27), potentially due to more intensive urbanisation—which exacerbates the urban heat island effect—and a higher prevalence of vulnerable populations, such as ageing residents (appendix p 28).⁴² Therefore, reducing temperature by the same degree might yield a greater reduction in mortality risks, leading to more pronounced benefits of greenness. In contrast, low-income areas might have a substantial heat-related mortality burden driven by behavioural patterns (eg, a higher likelihood of outdoor work),

greater physiological sensitivity (eg, pre-existing health conditions), and low adaptive capacity (eg, reduced access to cooling centres or air conditioning).^{41,43} These factors often have a more crucial role in heat vulnerability than EVI alone. Therefore, simply increasing greenness without addressing behavioural, physiological, and adaptive factors might not lead to a significant reduction in heat-related mortality in low-income areas. Third, the protective effect of greenness might be reduced in urban areas with low socioeconomic status, potentially due to differences in the quality or distribution of greenspaces.⁴⁴ Simply increasing the quantity of

greenness without ensuring accessibility might not effectively mitigate heat-related mortality risks, particularly if greenspaces are unevenly distributed or do not have features that promote effective heat mitigation.^{45–48} Further research is needed to better understand how the characteristics and spatial distribution of greenness influence its protective effects against heat-related mortality.

Despite these findings, the role of socioeconomic factors in the greenness–mortality association remains debated. A study in Switzerland reported that residential greenness had a higher protective effect on mortality risk in individuals with a higher socioeconomic status.⁴⁴ In contrast, another study suggested that increasing tree canopy coverage could prevent more premature deaths in areas with low socioeconomic status.⁴⁹ Future research could adopt diverse methodological approaches, such as longitudinal designs or quasi-experimental designs, to better assess how socioeconomic status, at both individual and community levels, shapes the relationship between greenness and heat-related mortality. Moreover, the interaction between socioeconomic status and other determinants, such as access to health care, climate adaptation strategies, and urban planning policies, would provide a more comprehensive understanding of this association.

The findings of our study provide insights for policy development. First, our research highlights the potential of increasing greenness as an effective strategy to reduce heat-related mortality. Increasing greenspace coverage in urban environments remains challenging due to constraints such as scarce space, high population density, and existing infrastructure constraints. However, this study reveals that a moderate increase in greenness could reduce heat-related mortality burden through its cooling effects on temperature and modifying effects on heat-related mortality risk. Therefore, integrating greenness into urban planning and adaptation strategies is essential. Measures could include expanding existing greenness areas,¹² promoting green roofs and walls,⁵⁰ and incorporating greenspaces into redeveloped projects.⁵¹ Additionally, increasing greenness can provide co-benefits, such as flood risk mitigation, improved air quality, reduced chronic disease rates, and enhanced psychological wellbeing.⁵² However, it should also be noted that for urban areas with the highest greenness levels, further increases in greenness might yield limited benefits. Second, our findings indicate that the cooling effects of greenness might vary across urban areas with different characteristics. Over the past two decades, cities in the Global North have seen a greater increase in greenness compared with cities in the Global South.⁵³ Rapid urbanisation in low-income and middle-income countries has often led to substantial environmental degradation, including the replacement of greenspaces with built-up land.^{53,54} This pattern suggests that efforts to enhance heat resilience

in less developed regions might have challenges. Our study emphasises the need to combine poverty alleviation efforts with other measures, such as heat warning systems, improved building design and passive cooling systems, broader access to public health services, and mental health support, to strengthen adaptive capacity in these regions.^{55,56}

This study has several strengths. This study uniquely assesses both the cooling effect of greenness on temperature and its modifying effect on heat–mortality risk, thereby providing a comprehensive assessment of the potential reduction in heat-related mortality burden due to greenness. The findings can help to develop tailored strategies against global warming at the national or subnational level. Additionally, we used uniform analytical approaches to assess the effect modification of greenness on the exposure–response relationship across all locations, ensuring the robustness and comparability of our results.

Several limitations should be acknowledged. We assumed that the mortality rate is identical across urban areas within the same country due to the absence of urban-specific mortality rate data. However, this is a common assumption in the global burden of disease studies.^{57,58} This study did not characterise the benefits of greenness across age and sex groups due to the absence of age-specific and sex-specific mortality data at both the location and urban area level. Future research would complement our findings if such data were to become available. We extrapolated the heat–mortality association to each urban area based on heat–mortality associations from 830 locations in 53 countries. Although these locations cover a wide range of climatic, demographic, and socioeconomic characteristics, the interpretation of our findings for Africa should be taken with caution, as there is scarce information from the MCC Collaborative Research Network in this region. Similarly, as only five locations from Oceania were included, the eCIs of attributable fractions of heat-related deaths are wide, suggesting high uncertainty in the estimates. Further studies are needed to validate these findings and explore the underlying mechanisms. Furthermore, we did not differentiate between types of greenness (eg, trees or grass) in this study, although various vegetation types could have distinct cooling effects on ambient temperatures, such as differences in modifying humidity and water vapour.⁵⁹ Additionally, small-scale greenspaces, such as street trees or pocket parks, might not be fully captured in this study due to the coarse resolution of EVI (250 m). Future studies should explore how specific vegetation types contribute to heat mitigation and incorporate higher-resolution satellite data, by combining the local characteristics, to better capture fine-scale greenness variations in urban environments.

In conclusion, our study provides the first global assessment of the potential reduction in heat-related

mortality burden due to an increase in greenness. We estimated that increasing EVI has a cooling effect on temperature and significantly reduces heat-related mortality risk. Consequently, increasing EVI is expected to result in a substantial decrease in heat-related mortality burden across the globe, particularly in several hotspots (ie, South Asia, East Europe, and East Asia). Preserving and expanding greenness should be incorporated into adaptation strategies to mitigate the health impacts of heat exposure.

MCC Collaborative Research Network

Ala Overcenco, Aleš Urban, Alexandra Schneider, Alireza Entezari, Ana Maria Vicedo-Cabrera, Antonella Zanobetti, Antonis Analitis, Aurelio Tobias, Baltazar Nunes, Barrak Alahmad, Bertil Forsberg, Carmen Íñiguez, Caroline Ameling, César De la Cruz Valencia, Christofer Åström, Danny Houthuijs, Do Van Dung, Ene Indermitte, Fatemeh Mayvaneh, Fiorella Acquafatta, Gabriel Carrasco-Escobar, Haidong Kan, Hanne Krage Carlsen, Hans Orru, Ho Kim, Iulian-Horia Holobaca, Jan Kyselý, Jouni J K Jaakkola, Klea Katsouyanni, Magali Hurtado Diaz, Martina S Ragetti, Masahiro Hashizume, Micheline de Sousa Zanotti Stagliorio Coelho, Nicolás Valdés Ortega, Noah Scovronick, Paola Michelozzi, Patricia Matus Correa, Patrick Goodman, Paulo Hilario Nascimento Saldiva, Raanan Raz, Rosana Abrutzky, Samuel Osorio, Shih-Chun Pan, Shilpa Rao, Tran Ngoc Dang, Valentina Colistro, Veronika Huber, Whanhee Lee, Xerxes Seposo, Yasushi Honda, Yoonhee Kim, Yue Leon Guo.

Contributors

YG and SL conceived the study and designed the methodology. YW performed the methodology and analysis, produced the original figures, and drafted the manuscript. BW, TY, and YL contributed to the methodology. All authors provided the data and contributed to interpretation of the results and revised the manuscript. YG, SL, and YW accessed and verified the data. All authors had full access to all the data in the study and had final responsibility for the decision to submit for publication.

Declaration of interests

YW, BW, TY, and WH were supported by China Scholarship Council grants (202006010044, 202006010043, 201906320051, and 202006380055). SL was supported by an Emerging Leader Fellowship (GNT2009866) of the Australian National Health and Medical Research Council. YG was supported by a Leader Fellowship (GNT2008813) of the Australian National Health and Medical Research Council. All other authors declare no competing interests.

Data sharing

Data have been collected within the Multi-Country Multi-City (MCC) Collaborative Research Network (<https://mccstudy.lshtm.ac.uk/>) under a data sharing agreement and cannot be made publicly available. Researchers can refer to MCC participants listed as coauthors for information on accessing the data for each country.

Acknowledgments

This study was supported by Australian Research Council (DP210102076), and Australian National Health and Medical Research Council (GNT2000581).

References

- Weinberger KR, Harris D, Spangler KR, Zanobetti A, Wellenius GA. Estimating the number of excess deaths attributable to heat in 297 United States counties. *Environ Epidemiol* 2020; **4**: e096.
- Gasparrini A, Guo Y, Hashizume M, et al. Temporal variation in heat-mortality associations: a multicountry study. *Environ Health Perspect* 2015; **123**: 1200–07.
- Vicedo-Cabrera AM, Scovronick N, Sera F, et al. The burden of heat-related mortality attributable to recent human-induced climate change. *Nat Clim Chang* 2021; **11**: 492–500.
- Masselot P, Mistry M, Vanoli J, et al. Excess mortality attributed to heat and cold: a health impact assessment study in 854 cities in Europe. *Lancet Planet Health* 2023; **7**: e271–81.
- Zhao Q, Guo Y, Ye T, et al. Global, regional, and national burden of mortality associated with non-optimal ambient temperatures from 2000 to 2019: a three-stage modelling study. *Lancet Planet Health* 2021; **5**: e415–25.
- Yang J, Zhou M, Ren Z, et al. Projecting heat-related excess mortality under climate change scenarios in China. *Nat Commun* 2021; **12**: 1039.
- Gasparrini A, Guo Y, Sera F, et al. Projections of temperature-related excess mortality under climate change scenarios. *Lancet Planet Health* 2017; **1**: e360–67.
- Iungman T, Cirach M, Marando F, et al. Cooling cities through urban green infrastructure: a health impact assessment of European cities. *Lancet* 2023; **401**: 577–89.
- Smith IA, Fabian MP, Hutyrá LR. Urban green space and albedo impacts on surface temperature across seven United States cities. *Sci Total Environ* 2023; **857**: 159663.
- Xu C, Chen G, Huang Q, et al. Can improving the spatial equity of urban green space mitigate the effect of urban heat islands? An empirical study. *Sci Total Environ* 2022; **841**: 156687.
- Yao L, Li T, Xu MX, Xu Y. How the landscape features of urban green space impact seasonal land surface temperatures at a city-block-scale: an urban heat island study in Beijing, China. *Urban For Urban Green* 2020; **52**: 126704.
- Choi HM, Lee W, Roye D, et al. Effect modification of greenness on the association between heat and mortality: a multi-city multi-country study. *EBioMedicine* 2022; **84**: 104251.
- Burkart K, Meier F, Schneider A, et al. Modification of heat-related mortality in an elderly urban population by vegetation (urban green) and proximity to water (urban blue): evidence from Lisbon, Portugal. *Environ Health Perspect* 2016; **124**: 927–34.
- Ma W, Chen R, Kan H. Temperature-related mortality in 17 large Chinese cities: how heat and cold affect mortality in China. *Environ Res* 2014; **134**: 127–33.
- Dang TN, Van DQ, Kusaka H, Seposo XT, Honda Y. Green space and deaths attributable to the urban heat island effect in Ho Chi Minh City. *Am J Public Health* 2018; **108**: S137–43.
- Schinasi LH, Bakhtsiyarava M, Sanchez BN, et al. Greenness and excess deaths from heat in 323 Latin American cities: do associations vary according to climate zone or green space configuration? *Environ Int* 2023; **180**: 108230.
- Guo Y, Gasparrini A, Armstrong B, et al. Global variation in the effects of ambient temperature on mortality: a systematic evaluation. *Epidemiology* 2014; **25**: 781–89.
- Schiavina M, Melchiorri M, Pesaresi M. GHS-SMOD R2023A—GHS settlement layers, application of the Degree of Urbanisation methodology (stage I) to GHS-POP R2023A and GHS-BUILT-S R2023A, multitemporal (1975–2030). 2023. https://human-settlement.emergency.copernicus.eu/ghs_smod2023.php (accessed June 10, 2024).
- Eurostat. Applying the degree of urbanisation—a methodological manual to define cities, towns and rural areas for international comparisons—2021 edition. 2021. <https://ec.europa.eu/eurostat/web/products-manuals-and-guidelines/-/ks-02-20-499> (accessed June 1, 2024).
- Didan K. MOD13Q1 MODIS/Terra vegetation indices 16-day L3 global 250m SIN grid V006. 2015. <https://ladsweb.modaps.eosdis.nasa.gov/missions-and-measurements/products/MOD13Q1> (accessed June 10, 2024).
- Huete A, Justice C, Van Leeuwen W. MODIS vegetation index (MOD13). 1999. https://modis.gsfc.nasa.gov/data/atbd/atbd_mod13.pdf (accessed June 10, 2024).
- Huete A, Didan K, Miura T, Rodriguez EP, Gao X, Ferreira LG. Overview of the radiometric and biophysical performance of the MODIS vegetation indices. *Remote Sens Environ* 2002; **83**: 195–213.
- Muñoz Sabater J. ERA5-Land hourly data from 1950 to present. 2019. <https://cds.climate.copernicus.eu/datasets/reanalysis-era5-land?tab=download> (accessed June 2, 2024).
- Wu Y, Li S, Zhao Q, et al. Global, regional, and national burden of mortality associated with short-term temperature variability from 2000–19: a three-stage modelling study. *Lancet Planet Health* 2022; **6**: e410–21.
- Zhou L, He C, Kim H, et al. The burden of heat-related stroke mortality under climate change scenarios in 22 East Asian cities. *Environ Int* 2022; **170**: 107602.

- 26 Zhao Q, Li S, Ye T, et al. Global, regional, and national burden of heatwave-related mortality from 1990 to 2019: a three-stage modelling study. *PLoS Med* 2024; **21**: e1004364.
- 27 Rubel F, Brugger K, Haslinger K, Auer I. The climate of the European Alps: shift of very high resolution Köppen–Geiger climate zones 1800–2100. *Meteorol Z* 2017; **26**: 115–25.
- 28 Rubel F, Kottek M. Observed and projected climate shifts 1901–2100 depicted by world maps of the Köppen–Geiger climate classification. *Meteorol Z* 2010; **19**: 135–41.
- 29 Vicedo-Cabrera AM, Sera F, Gasparrini A. Hands-on tutorial on a modeling framework for projections of climate change impacts on health. *Epidemiology* 2019; **30**: 321–29.
- 30 He Y, Cheng L, Bao J, et al. Geographical disparities in the impacts of heat on diabetes mortality and the protective role of greenness in Thailand: a nationwide case-crossover analysis. *Sci Total Environ* 2020; **711**: 135098.
- 31 He F, Wei J, Dong Y, et al. Associations of ambient temperature with mortality for ischemic and hemorrhagic stroke and the modification effects of greenness in Shandong Province, China. *Sci Total Environ* 2022; **851**: 158046.
- 32 Denpetkul T, Phosri A. Daily ambient temperature and mortality in Thailand: estimated effects, attributable risks, and effect modifications by greenness. *Sci Total Environ* 2021; **791**: 148373.
- 33 Wang K, Zhao DS, Zhu Y, et al. Albedo-dominated biogeophysical warming effects induced by vegetation restoration on the Loess Plateau, China. *Ecol Indic* 2023; **154**: 154.
- 34 Bathiany S, Claussen M, Brovkin V, Raddatz T, Gayler V. Combined biogeophysical and biogeochemical effects of large-scale forest cover changes in the MPI earth system model. *Biogeosciences* 2010; **7**: 1383–99.
- 35 Li HW, Zhao YL, Wang CH, Ürge-Vorsatz D, Carmeliet J, Bardhan R. Cooling efficacy of trees across cities is determined by background climate, urban morphology, and tree trait. *Commun Earth Environ* 2024; **5**: 754.
- 36 Xu R, Li Y, Teuling AJ, et al. Contrasting impacts of forests on cloud cover based on satellite observations. *Nat Commun* 2022; **13**: 670.
- 37 Qiu C, Ji JS, Bell ML. Effect modification of greenness on temperature-mortality relationship among older adults: a case-crossover study in China. *Environ Res* 2021; **197**: 111112.
- 38 Watanabe H, Sugi T, Saito K, Nagashima K. Mechanism underlying the influence of humidity on thermal comfort and stress under mimicked working conditions. *Physiol Behav* 2024; **285**: 114653.
- 39 Zanobetti A, O'Neill MS, Gronlund CJ, Schwartz JD. Susceptibility to mortality in weather extremes: effect modification by personal and small-area characteristics. *Epidemiology* 2013; **24**: 809–19.
- 40 Kovach MM, Konrad CE 2nd, Fuhrmann CM. Area-level risk factors for heat-related illness in rural and urban locations across North Carolina, USA. *Appl Geogr* 2015; **60**: 175–83.
- 41 Gronlund CJ. Racial and socioeconomic disparities in heat-related health effects and their mechanisms: a review. *Curr Epidemiol Rep* 2014; **1**: 165–73.
- 42 Taylor J, Wilkinson P, Davies M, et al. Mapping the effects of urban heat island, housing, and age on excess heat-related mortality in London. *Urban Clim* 2015; **14**: 517–28.
- 43 Xu R, Zhao Q, Coelho MSZS, et al. Socioeconomic level and associations between heat exposure and all-cause and cause-specific hospitalization in 1,814 Brazilian cities: a nationwide case-crossover study. *PLoS Med* 2020; **17**: e1003369.
- 44 Vienneau D, de Hoogh K, Faeh D, Kaufmann M, Wunderli JM, Rössli M. More than clean air and tranquillity: residential green is independently associated with decreasing mortality. *Environ Int* 2017; **108**: 176–84.
- 45 Ekkel ED, de Vries S. Nearby green space and human health: evaluating accessibility metrics. *Landsc Urban Plan* 2017; **157**: 214–20.
- 46 James P, Banay RF, Hart JE, Laden F. A review of the health benefits of greenness. *Curr Epidemiol Rep* 2015; **2**: 131–42.
- 47 Geary RS, Thompson D, Mizén A, et al. Ambient greenness, access to local green spaces, and subsequent mental health: a 10-year longitudinal dynamic panel study of 2·3 million adults in Wales. *Lancet Planet Health* 2023; **7**: e809–18.
- 48 Tang MM, Li XW. The disparity of greenness accessibility across major metropolitan areas in the United States from 2013 to 2022. *Land* 2024; **13**: 1182.
- 49 Kondo MC, Mueller N, Locke DH, et al. Health impact assessment of Philadelphia's 2025 tree canopy cover goals. *Lancet Planet Health* 2020; **4**: e149–57.
- 50 Mabon L, Kondo K, Kanekiyo H, Hayabuchi Y, Yamaguchi A, Fukuoka: adapting to climate change through urban green space and the built environment? *Cities* 2019; **93**: 273–85.
- 51 Haaland C, van den Bosch CK. Challenges and strategies for urban green-space planning in cities undergoing densification: a review. *Urban For Urban Green* 2015; **14**: 760–71.
- 52 Kingsley M. Commentary—climate change, health and green space co-benefits. *Health Promot Chronic Dis Prev Can* 2019; **39**: 131–35.
- 53 Wu S, Chen B, Webster C, Xu B, Gong P. Improved human greenspace exposure equality during 21st century urbanization. *Nat Commun* 2023; **14**: 6460.
- 54 Chen Y, Yue W, La Rosa D. Which communities have better accessibility to green space? An investigation into environmental inequality using big data. *Landsc Urban Plan* 2020; **204**: 103919.
- 55 Pörtner HO, Roberts DC, Adams H, et al. Climate change 2022: impacts, adaptation and vulnerability. IPCC, 2022.
- 56 Leichenko R, Silva JA. Climate change and poverty: vulnerability, impacts, and alleviation strategies. *Wiley Interdiscip Rev Clim Change* 2014; **5**: 539–56.
- 57 GBD 2015 Mortality and Causes of Death Collaborators. Global, regional, and national life expectancy, all-cause mortality, and cause-specific mortality for 249 causes of death, 1980–2015: a systematic analysis for the Global Burden of Disease Study 2015. *Lancet* 2016; **388**: 1459–544.
- 58 Rudd KE, Johnson SC, Agesa KM, et al. Global, regional, and national sepsis incidence and mortality, 1990–2017: analysis for the Global Burden of Disease Study. *Lancet* 2020; **395**: 200–11.
- 59 Armson D, Stringer P, Ennos AR. The effect of tree shade and grass on surface and globe temperatures in an urban area. *Urban For Urban Green* 2012; **11**: 245–55.